Author(s): Rinaldi, R. & Mangino, R. & Cingolani, R. & Lipsanen, Harri & Sopanen, M. & Tulkki, J. & Braskén, M. & Ahopelto, J.

Title: Magneto-optical properties of strain-induced InxGa1-xAs parabolic quantum dots

Year: 1998

Version: Final published version

Please cite the original version:

Rinaldi, R. & Mangino, R. & Cingolani, R. & Lipsanen, Harri & Sopanen, M. & Tulkki, J. & Braskén, M. & Ahopelto, J. 1998. Magneto-optical properties of strain-induced InxGa1-xAs parabolic quantum dots. Physical Review B. Volume 57, Issue 16. P. 9763-9769. ISSN 1098-0121 (printed). DOI: 10.1103/physrevb.57.9763.

Magneto-optical properties of strain-induced $In_xGa_{1-x}As$ parabolic quantum dots

R. Rinaldi, R. Mangino, and R. Cingolani
Istituto Nazionale di Fisica della Materia, Unità di Lecce, Dipartimento di Scienza dei Materiali, Università di Lecce, 73100 Lecce, Italy

H. Lipsanen, M. Sopanen, and J. Tulkki
Optoelectronics Laboratory, Helsinki University of Technology, Otakaari 7A, P.O. Box 3000, FIN-02015 HUT, Finland

M. Braskeń
Department of Physics, Åbo Akademi University, 20500 Turku, Finland

J. Ahopelto
VTT Electronics, Tekniikantie 17, P.O. Box 1101, FIN-02044 VTT, Finland
(Received 30 July 1997; revised manuscript received 26 November 1997)

We have investigated the Zeeman splitting in strained $In_xGa_{1-x}As$ quantum dots with different quantization energies by means of magnetoluminescence. A multifold splitting of Π and Δ states is observed due to lifted degeneracy of $m>0$ states. The experimental data were systematically compared to the diamagnetic and Zeeman shift of the single-particle states, taking into account the details of the valence-band structure and the spin splitting. Our data indicate that excitonic effects are negligible and that the magneto-optical properties of these strongly confined dots can be described rather accurately within the single-particle model. [S0163-1829(98)02116-X]

I. INTRODUCTION

In the last five years great attention has been devoted to the problem of artificial atoms in a magnetic field. Artificial atoms can be obtained by confining the electron motion along three directions in semiconductor nanostructures of lateral dimensions comparable to the de Broglie wavelength of the material. These systems are known as quantum dots or zero-dimensional nanostructures (0DNS). The energy spectrum of the 0DNS is a sequence of δ-like states centered at the eigenstate energies, resembling the discrete spectrum of atoms. Despite the important properties that differentiate the artificial atoms from the natural atoms (electron effective mass, screening of the repulsive electron-electron interaction via the effective dielectric constant,[1–3] nonsingular character of the confining potential, etc.), the study of macroatoms in high magnetic fields elucidates several interesting effects that are very similar to those studied by classical atomic physics. For instance, it has been demonstrated that the magnetic interaction in artificial atoms with axially symmetric potential causes the lifting of the degeneracy of states having different values of the angular momentum quantum number, resulting in the formation of the so-called Darwin-Fock states.[4,5] This effect is similar to the Zeeman splitting occurring in the electronic states of real atoms, thus reinforcing the analogy between quantum dots and atoms.[6]

Although this finding is quite clear in itself, the actual description of the magnetic interactions in mesoscopic systems is still unclear. Unlike the case of real atoms, quantum dots can be realized by different methods, namely, direct patterning of heterostructures, self-organization, and field-effect confinement, so that only electrons or both electrons and holes can be confined in the structure. In the former case, which is typical of field-effect quantum dots, the magnetic-field evolution of the quantized levels is dominated by the electron-electron correlation and has been theoretically[2,3,7,8] and experimentally investigated[9–11] in some detail in recent years.

Conversely, the successful realization of high-quality self-organized dots has recently allowed the study of macroatoms where both electrons and holes are confined in the respective 0D subbands, so that the electron-hole correlation is expected to be quite relevant.[12] The extent to which the Coulomb interaction affects the energy spectrum of the dots as compared to the confinement energy and to the magnetic interaction is still a matter of debate.[13–15]

In order to contribute to the understanding of this important point, we have studied the magnetic-field dependence of the Zeeman splitting and of the diamagnetic shift observed in the magnetoluminescence spectra of different parabolic quantum dots of excellent structural quality. Our attention has been devoted to the competition between the magnetic energy and the Coulomb energy in quantum dots with substantially different confinement energies ($\hbar\omega_0$, where ω_0 is the eigenfrequency of the circular oscillator). The comparison of the experimental spectra with the theory indicates that excitonic effects (electron-hole correlation) are in most cases negligible, and that a single-particle picture accounts well for the measured Zeeman splitting and diamagnetic shift of the interband transitions. The paper is organized as follows: In Sec. II we give some details on the growth conditions and on the structural characteristics of the investigated samples; in Sec. III we present our experimental and theoretical results and discuss the optical properties of the $In_xGa_{1-x}As$ quantum dots under an external magnetic field. Our conclusions are drawn in Sec. IV.

II. EXPERIMENT

The samples were grown by metal-organic vapor phase epitaxy at atmospheric pressure. The layers were deposited at 650 °C in a single growth run on semi-insulating (100)

TABLE I. Nominal values of the $In_xGa_{1-x}As$ quantum well thickness L_z in nm, of the GaAs space layer thickness d in nm, of the In content x. ΔE is the transition energy spacings (see text).

Sample	L_z (nm)	d (nm)	x	ΔE (meV)
A	8	20	0.08	10.5
B	8	20	0.20	13.6
C	8	5	0.08	14
D	8	5	0.20	11.7
E	8	5	0.25	14.25
F[a]	8	5	0.25	20.35

[a]Reference 19.

$\pm 0.5°$ GaAs substrates without intentional doping. Sources were trimethylgallium, trimethylindium, tertiarybutylarsine, and tertiarybutylphosphine. The quantum dot consists of an $In_xGa_{1-x}As$ quantum well (QW) buried by a GaAs top barrier of thickness d. Self-organized InP islands (stressors) are grown on the GaAs surface in order to induce a suitable strain potential that laterally confines the carriers in the $In_xGa_{1-x}As$ QW underneath the stressor. In Table I we report the width I_z of the $In_xGa_{1-x}As$ QW, the In content x, and the top barrier width d of the samples investigated in this paper. The growth rate and V/III ratio for GaAs and $In_xGa_{1-x}As$ were about 1.5 ML/s and 40, respectively. The V/III ratio in the growth of InP was 100. The InP islands for the uniformity study were grown directly on the GaAs buffer with various growth rates. Atomic force microscopy was used to probe the surface of the samples, evidencing the good size uniformity of the self-organized InP stressors. Details on the samples can be found in Ref. 16.

The photoluminescence and magnetoluminescence measurements were performed in a cryostat equipped with a superconducting magnet providing fields up to 10 T at 2.2 K. The luminescence was excited by an argon-ion laser, dispersed by a single 1-m monochromator, and detected by a cooled Ge detector.

III. RESULTS AND DISCUSSION

A. Experimental results

In Fig. 1 we show the photoluminescence spectra of the investigated samples under low-power cw excitation. The high quality of the samples is evidenced by several excited states that contribute to the total emission spectra and by the sharpness of the transition lines (typical full width at half maximum FWHM are of the order of 5–6 meV at 4 K). These spectra indicate that the number of filled subbands and the strength of the recombination lines strongly depend on the depth of the lateral (parabolic) confining potential.[17,18] The lateral confinement energy primarily depends on the width of the InP stressor, on the thickness of the space layer d, and on the In content. Actually, the width of the InP islands is kept almost constant by the Stransky-Krastanov growth parameters, so that a proper tuning of the confinement energies is obtained by changing d and x.[19] Since the strain field is maximum at the interface between the InP islands and the GaAs surface and decays exponentially under the surface, the d parameter acts on both the height and the width of the parabolic potential.[17] On the other hand, the In content influences both the depth of the parabolic potential and the mass of the confined particles. By increasing the In content, the potential well gets deeper and the mass gets lighter, resulting in a stronger confinement for both electrons and holes. This is clearly reflected in the increased intersubband splitting observed in dots having small d values and large x values, as shown in Fig. 1.

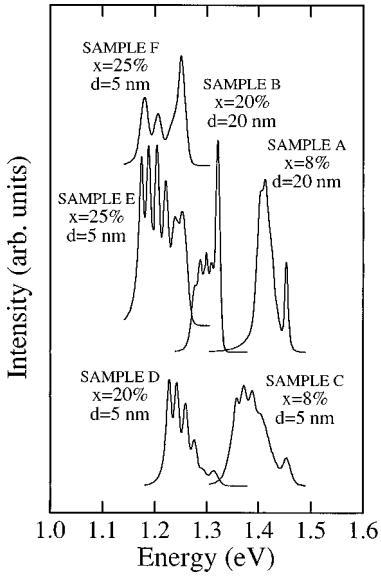

FIG. 1. Photoluminescence spectra of the investigated samples. $T=12$ K, $\lambda_{exc}=488$ nm, $I_{exc}=5$ W/cm^2.

The sharp interband recombination lines observed in the photoluminescence PL spectra allow us to deconvolute the spectra and to follow the temperature and intensity dependences of the individual transitions. This is done by fitting each transition line by a Gaussian line shape and by minimizing the χ^2 of the overall spectrum (Fig. 2). In the inset of Fig. 2 we show how this procedure provides the temperature dependence and the peak energies up to almost room temperature. Similarly, the line-shape fitting of the band filling spectra obtained under increasing photopumping intensities provides the intensity dependence of the strength of the various transitions. These simple deconvolutions are found to be quite accurate, thanks to the excellent signal-to-noise ratio of the spectra and to the smooth line shapes, and will be used below in order to extract the energy positions of the spectral features as a function of the magnetic-field flux.

In Fig. 3 we show the typical evolution of the PL spectra under a magnetic field perpendicular to the QW layer. The power density was set at $10\ \mathrm{W\,cm^{-2}}$ so as to have band filling spectra with several well-resolved transitions. The highest energy feature in these spectra is due to the recombination from the quantum well QW between adjacent dots.

The lifting of level degeneracy induced by the external magnetic field parallel to the z axis results in a very complex spectrum of eigenstates. With increasing the magnetic field the quantum dot lines corresponding to the excited states broaden and split into two or more lines of different amplitude and width depending on the value of the angular momentum quantum number.

From the line-shape analysis of the multitransition spectra we are able to draw the fan plots of the energies as a function

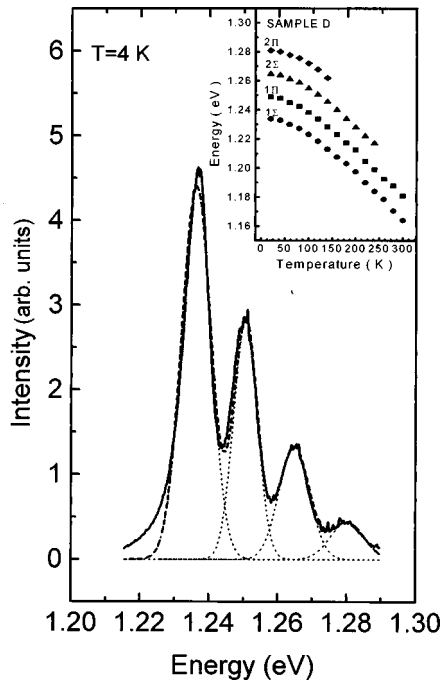

FIG. 2. Line-shape analysis of a typical PL spectrum at zero magnetic field by Gaussian deconvolution (sample D, $T=4$ K, $I_{\mathrm{exc}}=10$ W cm^{-2}). Inset shows temperature evolution of the ground and first three excited states of sample D.

of the magnetic field. All samples exhibit the lifting of degeneracy of the excited states (Zeeman effect), whereas the 1Σ state ($m=0$) does show only the usual diamagnetic shift. In a previous work,[6] we have already shown that the observed Zeeman splitting and diamagnetic shift can be quite satisfactorily described by a single-particle model, in the two band approximation. The Zeeman effect term is expected to increase linearly in the field[20] as

$$\Delta E_Z=\frac{e\hbar}{2m_0}\left(\frac{1}{m_r^e}+\frac{1}{m_r^h}\right)Bm, \tag{1}$$

where m_0 is the electron mass, $m_r^{e(h)}$ is the electron (hole) in-plane effective mass, and m is the value of the angular momentum quantum number ($m>0$). The diamagnetic shift coming from the quadratic B term in the Hamiltonian is evaluated starting from the magnetic-field dependence of the states with $m=0$ (Σ states):

$$\Delta E_D=\frac{e^2}{8m_0}\left(\frac{\langle r^2\rangle^e}{m_r^e}+\frac{\langle r^2\rangle^h}{m_r^h}\right)B^2. \tag{2}$$

Here the expectation values $\langle r^2\rangle^e$ and $\langle r^2\rangle^h$ are calculated with wave functions corresponding to nonzero external fields. In the case of free carriers we expect that the diamagnetic shift decreases with increasing the confinement potential, i.e., with reducing the spatial extent of the electron and hole wave functions. For almost equally confined samples the contribution of the effective mass becomes relevant and carriers confined in In-rich quantum dots (lighter masses) exhibit larger diamagnetic shifts. We have to mention that the presence of excitons should result in a diamagnetic shift substantially smaller than that of the single-particle states. It is therefore crucial to evaluate precisely the magnetic energy of electrons and holes in order to verify this qualitative indication.

B. Electronic states of parabolic quantum dots in a magnetic field

The qualitative analysis of the experimental data discussed in the previous section raises the question about the actual observability of Coulomb correlation effects in the magneto-optical spectra of our dots. In other words, the question is how Coulomb correlation can modify the single-particle spectra. Generally speaking, Coulomb correlation effects can be due to electron-electron or electron-hole interaction. Electron-electron correlation effects are not observable in these magnetoluminescence experiments because of the following.

(i) The temperature of the carriers in the cw experiments is higher than the sample temperature in the liquid He ($\simeq 4$ K) resulting in a broadened Fermi distribution. Correlation effects are indeed usually detected only for temperatures below 1 K as reported in Ref. 8.

(ii) The photoexcited number of electron-hole pairs at the typical excitation densities of Fig. 1 is of the order of 8–10 pairs per dot, resulting in the filling of the first five energy states. Because of the approximate charge neutrality of the dots this leads to a rapid screening of the electron-electron repulsion.

(iii) The broadening of quantum dot energy levels due to inhomogeneities of the self-organized island size (extrinsic or Gaussian broadening) and to the scattering processes due to hot carriers (intrinsic or Lorentian broadening) prevents the observation of a fine structure due to intraband correlation effects.

Experimentally, the lack of electron-electron interaction is confirmed by the intensity-dependent PL measurements shown in Fig. 4. The excitation intensity was increased from a few tens of mW/cm^2 up to 30 W/cm^2 in order to progressively fill the quantized states. By increasing the excitation intensity we observe neither shift of the transition lines nor splitting, indicating that electron-electron or hole-hole correlation effects do not influence our experimental observations. In the highest intensity PL spectra all five quantized levels of the dots are filled, so that 30 electron-hole (e-h) pairs can be assumed in each dot. Given the dot density of 2×10^9 cm^{-2}, this corresponds to a photogeneration rate of about 6×10^{10} cm^{-2} for the maximum excitation intensity at a temperature of 0 K. Actually, if we take into account the finite carrier temperature that is slightly higher than the crystal temperature (some 20–30 K) we can estimate that the number of e-h pairs in Fig. 4 ranges between 2 at the lowest power, about 20 at 10 W/cm^2, and about 30 at the maximum power. Most of the experiments shown in this paper have been performed with typically 8 e-h pairs at low density (three subbands observed in the PL spectra) or about 20 e-h pairs at the maximum power (five subbands in the PL spectra).

On the other hand, electron-hole correlation (excitonic effect) should not be observed because the exciton wave function in a strongly confined dot can be simply constructed by the product of the single-particle wave functions, which are

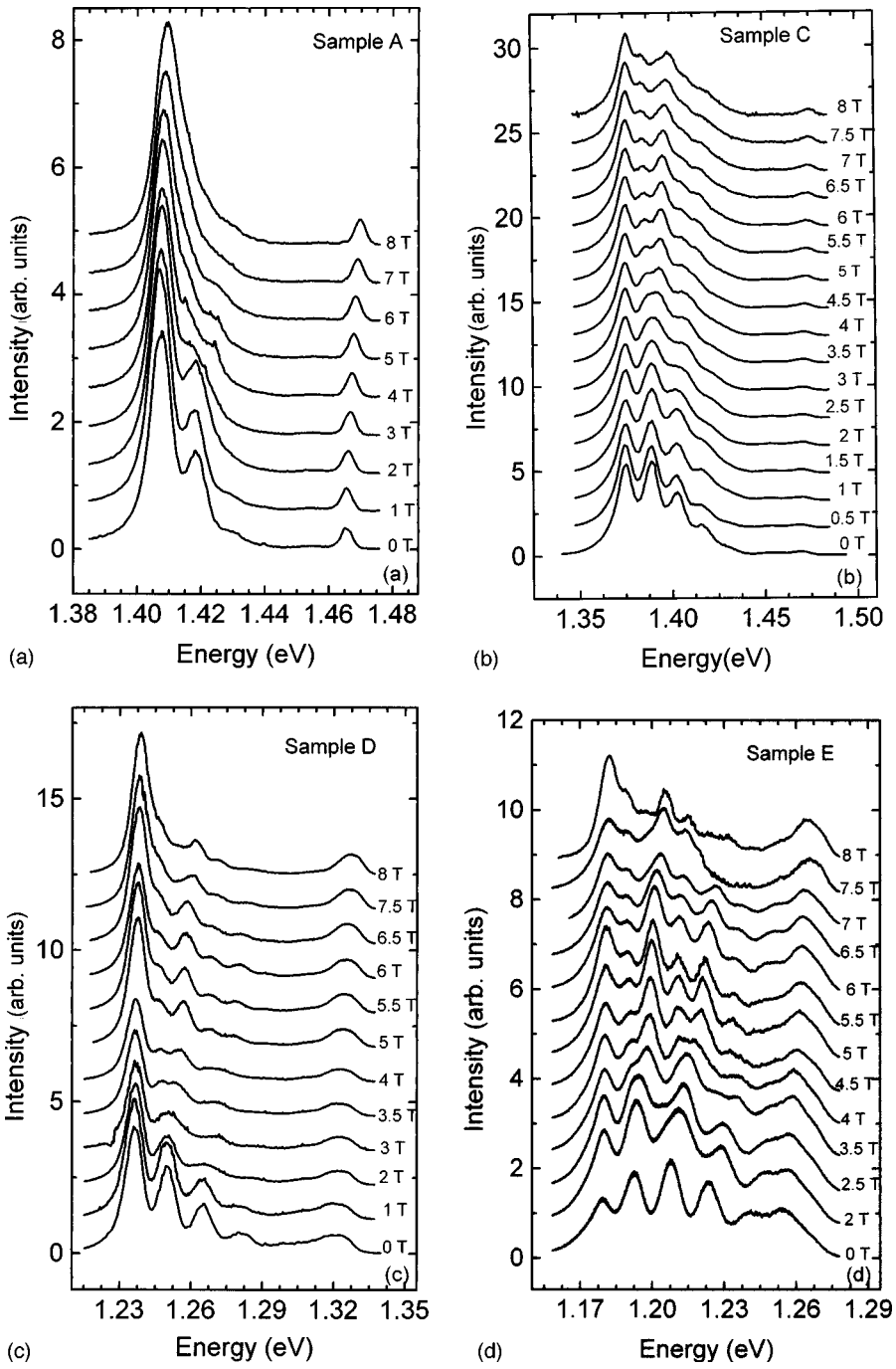

FIG. 3. (a)–(d) Magnetic-field-dependent luminescence spectra of samples *A*, *C*, *D*, and *E*, respectively, at 4 K. The magnetic-field direction is parallel to the growth axis.

strongly localized in the dot. The 1*s* orbital wave function (envelope function of the exciton) usually written for one- and two-dimensional systems, does not appear in this case due to the lack of degrees of freedom for the center-of-mass motion of the exciton particle in the dot.[21] Under this assumption, the magnetic interaction on the quantum dot excitons reduces to the magnetic interaction on the single-particle states, i.e., the electron and hole diamagnetic shift plus the Zeeman splitting. While this argument is clearly valid for quantum dots with very strong confinement, the calculation of Bockelmann[14] shows that for a parabolic quantum dot having a level spacing of 10.7 meV the magnetic dispersion is still governed by excitonic behavior and the first excited state luminescence peak does not exhibit any Zeeman splitting.

In order to test this hypothesis we have performed a full calculation of the diamagnetic shift and Zeeman splitting of the $1\Sigma^{\pm}$ and $1\Pi^{\pm}$ states in our samples, which includes the accurate valence-band description and the spin splitting of the single-particle states. The valence band was calculated by the four band Luttinger-Kohn method.[18,22] In short, the computational analysis includes the following stages: First, the strain distribution is calculated from the theory of elasticity by minimizing the total strain energy; a dislocation-free

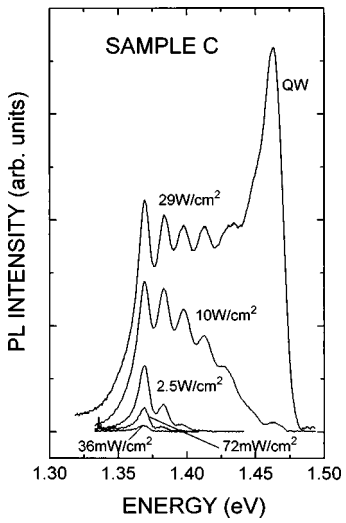

FIG. 4. Intensity-dependent PL spectra of sample *C* at 10 K.

structure is assumed. Second, the strain distribution is converted into deformation potentials using the theory of Pikus and Bir.[23] Finally, the confinement energies and envelope wave functions are calculated by the four band Luttinger-Kohn theory, including both the strain-induced confinement and the QW band-edge confinement.

Using minimal substitution, the Hamiltonian including the strain-induced confinement and the magnetic field[24] results in

$$H=\begin{pmatrix} H_{\rm hh}+V_{\rm hh} & b & c & 0 \\ b^{\dagger} & H_{\rm lh}+V_{\rm lh} & 0 & c \\ c^{\dagger} & 0 & H_{\rm lh}+V_{\rm lh} & -b \\ 0 & c^{\dagger} & -b^{\dagger} & H_{\rm hh}+V_{\rm hh} \end{pmatrix} + \frac{e}{m_0}\,\kappa B J_z, \tag{3}$$

where

$$H_{\rm hh,lh}=\frac{-\hbar^2}{2m_0}\left[(\gamma_1\mp 2\gamma_2)\,\frac{\partial^2}{\partial z^2} + (\gamma_1\pm\gamma_2)\left(\frac{\partial^2}{\partial x^2}+\frac{\partial^2}{\partial y^2}-2\,\frac{\overline{\omega}}{\hbar}\,\hat{L}_z-\overline{\omega}^2(x^2+y^2)\right)\right], \tag{4}$$

$$b=-\frac{\sqrt{3}\hbar^2}{m_0}\,\gamma_3\,\frac{\partial}{\partial z}\left(\frac{\partial}{\partial x}-i\,\frac{\partial}{\partial y}+\overline{\omega}(x-iy)\right), \tag{5}$$

$$c=\frac{\sqrt{3}\hbar^2}{2m_0}\,\frac{\gamma_2+\gamma_3}{2}\left(\frac{\partial}{\partial x}-i\,\frac{\partial}{\partial y}+\overline{\omega}(x-iy)\right)^2, \tag{6}$$

where m_0 is the bare electron mass and $\overline{\omega}=eB/2\hbar$. In Eq. (4) and below, the upper (lower) sign corresponds to heavy-hole (hh) band [light-hole (lh) band]. The nondiagonal terms of the Pikus-Bir strain Hamiltonian[23] were found to be small, especially for the few lowest states, and the hh and lh confinement potentials are given by $V_{\rm hh,lh}(r,z)=V_h^{\rm QW}(z)+V_h^H(r,z)\pm V_h^S(r,z)$, where $V_h^{\rm QW}(z)$ is the hole band-edge confinement potential, $V_h^H(r,z)=a_\nu(e_{xx}+e_{yy}+e_{zz})$ the hydrostatic deformation potential, and $V_h^S(r,z)=b_\nu[e_{zz}-(e_{xx}+e_{yy})/2]$ the shear deformation potential.

The z component of the total angular momentum is given by $\hat{J}_{\rm tot}=\hat{J}_z+\hat{L}_z$, where $\hat{L}_z$ is the mesoscopic angular momentum. The four component envelope function in cylindrical coordinates has the form $\psi_{m_j}(r,z,\phi)=e^{i(M-m_j)\phi}\chi_{m_j}(r,z)$, where $\hbar M$ is the eigenvalue of the z component of the total angular momentum and in the present case it is a good quantum number. M must be a positive or negative half-integer (but not an integer) and m_j takes the values $\pm 3/2$, $\pm 1/2$.

As discussed by Brasken, Lindberg, and Tulkki,[22] the mesoscopic angular momentum defined by the expectation value

$$\langle\hat{L}_z\rangle=\hbar\sum_{m_j}(M-m_j)\langle\chi_{m_j}|\chi_{m_j}\rangle \tag{7}$$

is approximately a constant of motion in *interband* transitions. Therefore, a mesoscopic angular momentum number m is a useful tool in identifying eigenstates from the experimental spectrum and we can label the valence-band states by $N\Sigma_{\uparrow\downarrow}, N\Pi^{\pm}_{\uparrow\downarrow}, N\Delta^{\pm}_{\uparrow\downarrow},\ldots$ in analogy to the electron states. The mesoscopic angular momentum number m is defined as the nearest integer to $\langle\hat{L}_z\rangle/\hbar$ and used as a label for the valence-band state.

The second quantity that has to be accounted for is spin splitting, which modifies the single-particle energy in a magnetic field depending on the spin orientation. We define the expectation value of spin for the valence band as

$$\langle\hat{S}_z\rangle=\frac{\hbar}{2}\left[-\langle\chi_{-3/2}|\chi_{-3/2}\rangle-\tfrac{1}{3}\langle\chi_{-1/2}|\chi_{-1/2}\rangle+\tfrac{1}{3}\langle\chi_{1/2}|\chi_{1/2}\rangle + \langle\chi_{3/2}|\chi_{3/2}\rangle\right]. \tag{8}$$

Whenever the $\chi_{\pm 3/2}$ component dominates we have $\langle\hat{S}_z\rangle\approx\pm 1/2\hbar$, respectively. We denote the dominant hh component by $\uparrow$ ($\downarrow$) for $m_j=3/2$ ($-3/2$). The numerical calculations showed that this leads to $m=M-3/2$ for the $\uparrow$ states and $m=M+3/2$ for the $\downarrow$ states. With this definition the spin is also approximately conserved in the dipole-allowed transitions. The strongest luminescence lines always correspond (excluding anticrossing regimes) to transitions between states having the same mesoscopic quantum number and spin.[25]

In Figs. 5(a)–5(d) we compare the magnetic shifts calculated by Eqs. (3)–(8) for the ground state 1Σ and the 1Π excited states (lines) with the experimental data (symbols). The agreement between the single-particle theory and the experiment is good for all the investigated samples. The onset of the experimental observation of the $1\Pi^{\pm}$ Zeeman splitting is shifted to higher fields with respect to the theoretical one because the Gaussian broadening of the transition lines prevents the detection of energy splitting smaller than 2.5 meV (approximately half-width of the emission line). Furthermore, the spin-up and spin-down splitting is found to be much less important than the Zeeman effect and is not resolved in the spectra.[26]

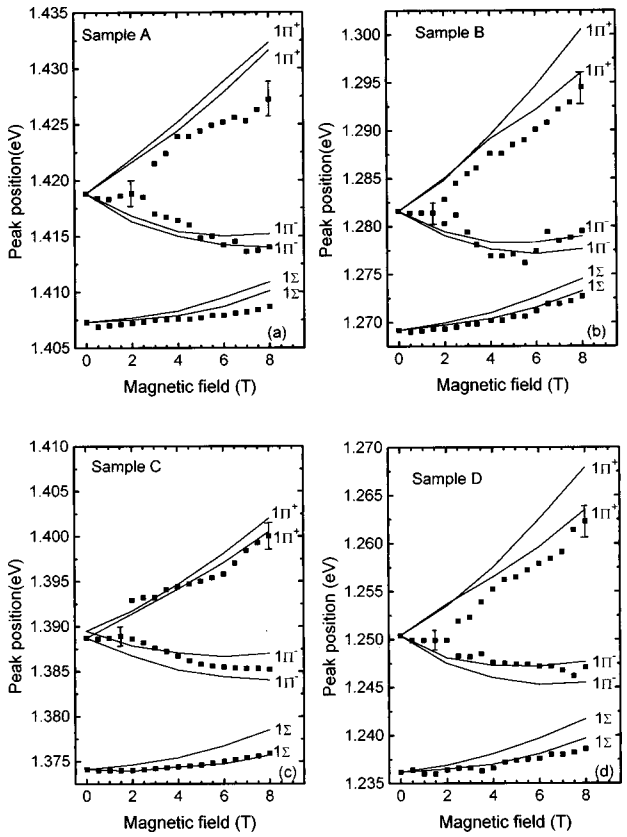

FIG. 5. Comparison between the calculated magnetic shifts of the 1Σ and 1Π transitions (lines) and the experimental data extracted from the magnetoluminescence spectra of samples *A*, *B*, *C*, and *D* (symbols). The error bars represent the best-fit error on the energy parameter obtained from the line-shape fitting. The error values are similar for all samples.

These data indicate the accuracy of the single-particle model for the quantitative analysis of the Zeeman effect in our parabolic quantum dots. The agreement between theory and experiment is found to be quite good in most samples with the exception of those having small confinement energies where the experimentally observed diamagnetic and Zeeman shifts are slightly smaller than the calculated ones. In this case some additional excitonic effect should be taken into account to improve the agreement between theory and experiment. We should note that in the case of weakly confined dots the electron-hole interaction is presumably reduced by the screening effect. Typically ten electron-hole pairs in a single quantum dot correspond to a carrier density of 10^{19} cm^{-3}, which is by far larger than the typical density for which screening of the Coulomb interaction becomes important. However, we have to mention that the *magnetoluminescence spectra collected under excitation intensities of the order of a few tens of* μW/cm^2 (i.e., *our detection limit*) *show the same diamagnetic shift and Zeeman splitting as the spectra recorded under much higher intensities*. The lack of any density dependence of the diamagnetic shift and Zeeman splitting somehow rules out the important role of screening. Our findings thus suggest that the single-particle picture describes quite well the magneto-optical properties of strongly confined quantum dots.

IV. CONCLUSIONS

In conclusion, we have studied the magneto-optical properties of strongly confined $In_xGa_{1-x}As$ parabolic quantum dots with intersubband spacing in the range between 10 and 27 meV. From the comparison between the experimentally observed and calculated diamagnetic shift and Zeeman splitting of confined states we can state that excitonic effects play a minor role in the magneto-optical properties of strongly confined dots and that a single-particle model describes quite well the emission properties of these strain-induced quantum dots.

ACKNOWLEDGMENTS

Two of us, R. Rinaldi and R. Cingolani, gratefully acknowledge Professor G. Bastard for enlightening discussions. The expert technical help of D. Cannoletta and A. Melcarne is gratefully acknowledged.

[1] W. Hansen *et al.*, Phys. Rev. Lett. **62**, 2168 (1989).
[2] P. Hawrylak, Phys. Rev. Lett. **71**, 3347 (1993).
[3] L. D. Hallam *et al.*, Phys. Rev. B **53**, 1452 (1996).
[4] C. G. Darwin, Proc. Cambridge Philos. Soc. **27**, 86 (1930).
[5] V. Fock, Z. Phys. **47**, 446 (1928).
[6] R. Rinaldi *et al.* Phys. Rev. Lett. **77**, 342 (1996).
[7] P. A. Maksym and T. Chakraborty, Phys. Rev. Lett. **65**, 108 (1990).
[8] W. Wagner *et al.*, Phys. Rev. B **45**, 1951 (1992).
[9] D. Heitmann, Physica B **212**, 201 (1995).
[10] Ch. Sikorski and U. Merkt, Phys. Rev. Lett. **62**, 2164 (1989).
[11] R. C. Ashoori, Phys. Rev. Lett. **71**, 613 (1993).
[12] W. Que, Phys. Rev. B **45**, 11 036 (1992).
[13] V. Halonen *et al.*, Phys. Rev. B **45**, 5980 (1992).
[14] U. Bockelmann, Phys. Rev. B **50**, 17 271 (1994).
[15] S. Jaziri and R. Bennaceur, Semicond. Sci. Technol. **9**, 1775 (1994).
[16] H. Lipsanen, M. Sopanen, and J. Ahopelto, Solid-State Electron. **40**, 601 (1996).
[17] H. Lipsanen *et al.*, Phys. Rev. B **51**, 13 868 (1995).
[18] J. Tulkki and A. Heinämäki, Phys. Rev. B **52**, 8239 (1995).
[19] In all the investigated samples, with the exception of sample *F*, the self-organized InP islands have rather constant size, with a height of 22 nm and a diameter of 80 nm. In sample *F* the islands were aggregated at a higher temperature, resulting in a smaller size.
[20] The selection rules for interband transitions are $\Delta n = 0$, $\Delta m = 0$; J. Pankove, *Optical Processes in Semiconductors* (Dover, New York, 1971).
[21] G. Bastard (private communication).
[22] M. Brasken, M. Lindberg, and J. Tulkki, Phys. Rev. B **55**, 9275 (1997).
[23] G. E. Pikus and G. L. Bir, Sov. Phys. Solid State **1**, 136 (1959).
[24] J. M. Luttinger and W. Kohn, Phys. Rev. **97**, 869 (1955); J. M.

Luttinger, *ibid.* **102**, 1030 (1956).

[25] Transitions that would correspond to an approximate spin flip are strictly forbidden because of the vanishing of the dipole moments. In contrast there is a finite probability for the change of the mesoscopic angular momentum in the luminescence emission, e.g., $I(1\Pi_{\downarrow}^{+} \rightarrow 1\Pi_{\downarrow}^{-}) = 0.003$.

[26] All the measurements were performed without changing the linear polarization of the exciting argon laser.